



## The doorsill of fullerene

Hui-Yan Zhao<sup>a,b</sup>, Ke-Min Liu<sup>a</sup>, Jing Wang<sup>a,b</sup>, Hui-Yun Han<sup>a</sup>, Ying Liu<sup>a,b,\*</sup>

<sup>a</sup> Department of Physics and Hebei Advanced Thin Film Laboratory, Hebei Normal University, Shijiazhuang 050024, Hebei, China

<sup>b</sup> National Key Laboratory for Materials Simulation and Design, Beijing 100083, China

### ARTICLE INFO

#### Article history:

Received 19 April 2012

In final form 10 November 2012

Available online 23 November 2012

### ABSTRACT

How difficult is it for a guest atom to cut through C<sub>60</sub> fullerene? Using an iron atom as a representative “intruder”, we explored the “quasistatic” processes of the atom going into and out from C<sub>60</sub> along 3-fold or 5-fold axis and investigated the geometrical, electronic structures, and energy changes in the processes. Encaging an iron atom through 3-fold axis was more favored, with a lower energy barrier of about 4.20 eV. As it moved into C<sub>60</sub> along 3-fold axis, the Fe atom must cross over two thresholds. The higher is located inside the C<sub>60</sub> but not the outside.

© 2012 Elsevier B.V. All rights reserved.

### 1. Introduction

Endohedral metallofullerene La@C<sub>60</sub> was first synthesized by the supersonic cluster-beam technique in the gas phase by Heath and co-workers in 1985 [1]. Since then, endohedral fullerenes have attracted much attention for their fascinating properties, novel electronic structures, and practical applications. In the past several years, endohedral metallofullerenes, with atoms such as La [2,3], Y [4,5], and Sc [6,7] encapsulated in C<sub>82</sub> or C<sub>84</sub> cages, have been confirmed using arc-desorption or laser vaporization techniques. Laser vaporization techniques have also revealed that alkali-metals such as K and Cs atoms can be trapped by the fullerene C<sub>60</sub> [2,8]. By radiochemical and radiochromatographic techniques, the radioactive endohedral fullerenes Be@C<sub>60</sub> [9], Xe@C<sub>60</sub> [10], and Po@C<sub>60</sub> [11] were detected by Ohtsuki and co-workers. Ohtsuki et al. [12,13] have also investigated the formation of fullerenes incorporating heavier atoms (Sb, Te, Se) by using radionuclides and *ab initio* molecular-dynamics simulations. Ion implantation has also been used to implant the non-metals N and P into a fullerene cage [14–16]. So far, it has been found that alkali metals, alkali-earth metals, transition metals, 3B–6B elements, nonmetallic elements, and noble elements can be doped into fullerene.

The electronic structures [17–21] and properties [22–29] of endohedral fullerenes have been intensively explored for their wide range of potential applications. Yang et al. [21], by systematically studying the electronic structure of endohedral metallofullerenes, have found that the charge transferred from the metal atom is highly localized inside the cage near the metal cations due to the strong metal–cage interactions rather than being uniformly distributed on the surfaces of the carbon cage as traditionally be-

lieved. Li et al. [29], using density functional theory (DFT), have performed calculations on the electronic and magnetic properties of a Mn atom encapsulated by a C<sub>60</sub> cage. They attribute the decrease in total energy and spin to hybridization of Mn and C electron orbitals. Endohedral fullerenes have some unique advantages because they can confine an atomic or molecular species within a shielded environment. For example, water soluble Gd-based metallofullerenes are considered as new candidates for magnetic resonance imaging contrast agents because they can produce greater proton relaxivities than available agents [30,31]. Moreover, the toxicity of Gd ions is completely isolated by the C<sub>60</sub> cage. More recently, Kurotobi and Murata [32] and Balch [33] reported that single water molecule is trapped within C<sub>60</sub> cage through a chemical process. C<sub>60</sub> cage creates a favorable environment to study water molecule at the fundamental level. In spite of the fundamental importance of understanding the formation process of endohedral fullerenes, most studies have focused on the preparation, properties, and electronic structure of endohedral fullerenes, with little effort devoted to the detailed formation process of encapsulating a guest atom or molecule in a fullerene cage.

In the present work, using Fe as a representative endohedral atom, we systematically investigate the quasi-static process of an atom entering or exiting from a C<sub>60</sub> cage. We also give a qualitative analysis of the energy barrier changes for these processes. Using a sequence of quasi-static states to study what is clearly a dynamic process cannot fully represent the formation and decay of molecules with encapsulated metal atoms, nevertheless it can be helpful for better understanding the broad picture of the formation of endohedral fullerenes.

### 2. Methods

This study follows an Fe atom approaching and eventually entering a C<sub>60</sub> fullerene cage along an axis through either a

\* Corresponding author at: Department of Physics and Hebei Advanced Thin Film Laboratory, Hebei Normal University, No. 20, East of South 2nd Ring Road, Shijiazhuang 050024, Hebei, China.

E-mail address: [yliu@hebtu.edu.cn](mailto:yliu@hebtu.edu.cn) (Y. Liu).

pentagon or hexagon face of  $C_{60}$  cage. This axis was chosen as the z-axis for the calculation. At several points along the trajectory of the Fe atom, the position of the atom was fixed and the geometrical structure of the cage was optimized in the presence of the Fe atom. In order to simplify the calculation, the z coordinate of the hexagon ( $C_6^{z\text{-fixed}}$ ) or pentagon ( $C_5^{z\text{-fixed}}$ ) farthest from the Fe atom was fixed at 0 in order to ensure that the C atoms on that side did not move in the z-direction during the optimization process. However, the movements of  $C_6^{z\text{-fixed}}$  or  $C_5^{z\text{-fixed}}$  are not constrained which clearly demonstrates that this calculation approach is feasible. A similar approach was also applied to study the exit of the Fe atom from the  $C_{60}$ .

The geometry optimization was performed to find the ground-state structure of the Fe +  $C_{60}$  system. A double-numeric-polarized (DNP) basis set without any spin constraints was chosen to carry out the electronic structure calculations. The Becke exchange plus Lee–Yang–Parr correlation (BLYP) [34] based on the generalized gradient approximation (GGA) was employed to take into account the exchange and correlation effects of electrons. In the optimizations, the energy gradient and atomic displacement were required to converge to  $1 \times 10^{-4}$  Hartree/Bohr and  $1 \times 10^{-4}$  Å, respectively. The self-consistent-field calculations were carried out with a convergence criterion of  $1 \times 10^{-6} e/\text{Å}^3$  for the charge density, which corresponds to a total energy convergence of  $1 \times 10^{-5}$  Hartree. All the calculations were carried out using all-electron DFT implemented in the DMol<sup>3</sup> package [35].

### 3. Results and discussion

By calculating the binding energy of the system at each point along the Fe trajectory, we found that given sufficient energy, the atom can penetrate into the  $C_{60}$  cage either through a hexagon ( $C_6^{\text{Right}}$ ) or a pentagon ( $C_5^{\text{Right}}$ ). However, the highest energy barrier for the path through a hexagon is at least about 4.20 eV lower than that for a pentagon, showing that penetration through a hexagon is favored. Therefore, in the present work, we have opted to focus our investigations on the processes where the atom enters or exits from the  $C_{60}$  cage along the axis through a hexagon.

For entering the  $C_{60}$ , the initial position of the atom relative to the center of the hexagon ( $C_6^{z\text{-fixed}}$ ) farthest from the Fe atom was taken to be about 9.50 Å. Here the atom is essentially a free atom. When the atom is far away from the center of  $C_6^{z\text{-fixed}}$ , the binding energy shows little variation, and the  $C_{60}$  cage almost retains its  $I_h$ -symmetry geometry, indicating a weak interaction between the atom and the cage. Referring to previous experimental studies treating the interaction between iron and fullerenes [36], it is found that the iron atom are weakly coordinated to the fullerene cage when the fullerene retains the neutral state with the  $I_h$  symmetry. Moreover, such weak coordinate is intermediate between Van der Waals contacts and strong Fe–C bonds. Fig. 1(a) gives the binding energy curve of the system as a function of separation. As the atom approaches the  $C_{60}$  cage, the energy begins to decline slightly when the distance between the atom and center of  $C_6^{z\text{-fixed}}$  is about 8.90 Å. As shown in Fig. 1(a), the energy variation is monotonic. This is a manifestation of weak coupling between Fe and cage. When the atom is about 8.27 Å away from  $C_6^{z\text{-fixed}}$ , the whole system of Fe +  $C_{60}$  achieves a relatively stable state with the binding energy reaching a minimum.

After the energy minimum, the energy, as shown in Fig. 1(a), increases gradually as the cage is compressed. This implies that the metal–cage interaction becomes repulsive and gets stronger and stronger as the atom moves towards the  $C_{60}$ . The energy reaches a local peak when the distance between the atom and  $C_6^{z\text{-fixed}}$  is about 7.21 Å, where the largest distortion occurs in the cage. After this point, the binding energy decreases rapidly to a local mini-

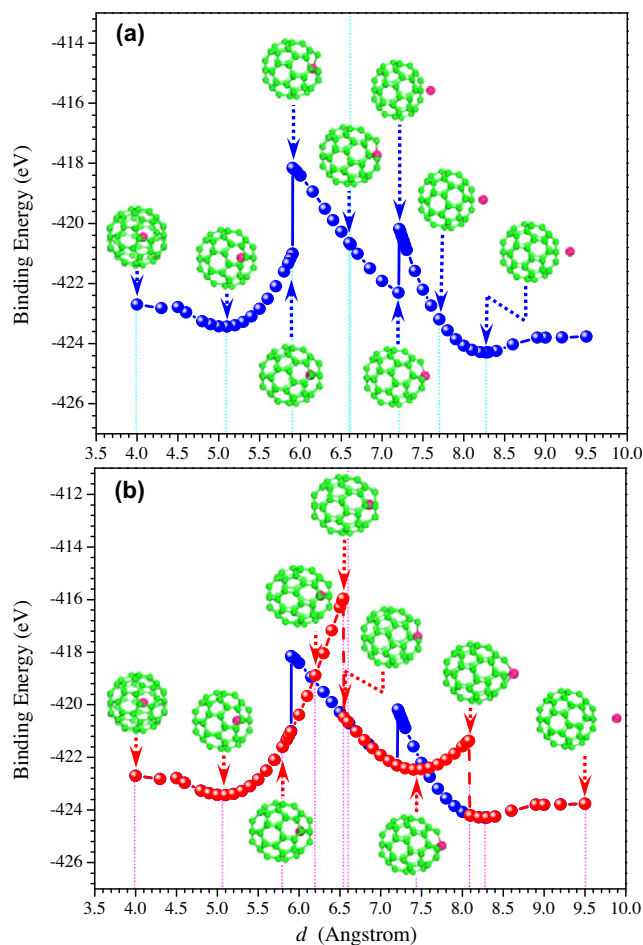


**Fig. 1.** Binding energy changes (eV) vs. distance  $d$  (Å) of the Fe atom relative to the center of the fixed hexagon ( $C_6^{z\text{-fixed}}$ ). (a) The plot with solid line is about the process of the atom going into  $C_{60}$ ; (b) the plot with dash line is about the process of the atom going out from  $C_{60}$ . The stable structures (small green ball: C; big pink ball: Fe) are also presented in some crucial positions of these processes. The vertical dot line denotes the position where the atom is located just in the plane of  $C_6^{\text{Right}}$ . (For interpretation of the references to color in this figure legend, the reader is referred to the web version of this article.)

um. Here it happens crossing the first threshold of Fe atom entering  $C_{60}$ . Referring to deformation densities of Fig. 2, it shows that the three C–C 5–6 bonds (pentagon–hexagon) are broken and that the Fe atom forms chemical bonds with the C atoms. The Fe–C bonding deforms the cage locally and moderately with a contraction of the C–C 6–6 bond length.

The formation of chemical bonds between the Fe atom and the C atoms results in a significant change in the distance between the Fe and the center of  $C_6^{\text{Right}}$ , as shown in Table 1. Both the charges transferred from the Fe atom to the cage and the spin moments of Fe (see Table 1) also show a significant decline with the rapid drop in the binding energy. The results are compared with those from the molecule  $C_{60}\text{CrC}_{60}$  where the  $\pi$  bonds on each side of the metal atom are localized on a hexagonal face of the fullerene [37]. It is found that the extra electronic flux resulting from the organometallic Fe–C bonds has enhanced the stability of the Fe +  $C_{60}$  system.

As the atom continues to move towards the center of the  $C_{60}$ , the binding energy begins to increase again due to the distortion of the Fe–C bonds. The highest energy barrier, 5.61 eV, taken here to be the energy with respect to that of the system when the Fe atom is far from the center of the cage, is reached when the atom is located at about 5.91 Å from the center of  $C_6^{z\text{-fixed}}$ . At this point, the atom is

Download English Version:

<https://daneshyari.com/en/article/5382601>

Download Persian Version:

<https://daneshyari.com/article/5382601>

[Daneshyari.com](https://daneshyari.com)